On the dense water in the Adriatic Sea

Bottom motion
Vein
Dense water
Adriatic Sea
Courant profond
Veine
Eau dense
Mer Adriatique

Antonio ARTEGIANI [a], **Roberto AZZOLINI** [a], **Ettore SALUSTI** [b]
[a] Istituto di Ricerca sulla Pesca Marittima, Consiglio Nazionale delle Rizerche, Ancona, Italy.
[b] Istituto Nazionale Fisica Nucleare, Dipartimento di Fisica, Università "La Sapienza", Roma, Italy.

Received 4/1/88, in revised form 8/8/88, accepted 29/8/88.

ABSTRACT

Historical data are used to investigate the formation and evolution of dense water in the Adriatic Sea. This dense water is of particular interest since, during its motion, it mixes with Intermediate Water of Levantine origin and comes to constitute one of the main sources of the bottom waters in the Eastern Mediterranean. In particular, we examine the periods and sites of formation, the time-evolution, the collapse into the Middle Adriatic Pit (Pomo or Jabuka Pit) and the overflow into the Southern Adriatic Pit of three types of dense water, with $\sigma > 29.2$, 29.4, 29.6 respectively, formed in winter in the Northern Adriatic. This dense water flows downward along the Italian coast with complex dynamics: it is influenced both by the bottom topography, particularly at the Middle Adriatic Pit and at the Southern Adriatic Pit, and by interaction with Intermediate Water.

Oceanologica Acta, 1989, **12**, 2, 151-160.

RÉSUMÉ

L'eau dense en Mer Adriatique

L'eau dense de la Mer Adriatique présente un intérêt particulier, car elle se mélange à l'eau intermédiaire d'origine levantine pour former l'une des principales sources d'eau de fond de la Méditerranée orientale. A partir de données historiques, le présent travail examine les zones et les périodes de formation de cette eau, son évolution et son écoulement dans la fosse centrale de l'Adriatique (fosse Pomo ou Jabuka), puis le déversement dans la fosse méridionale de l'Adriatique de trois types d'eaux denses ($\sigma > 29,2$; 29,4 et 29,6 respectivement), formées en hiver dans le nord de l'Adriatique. Le mécanisme de plongée de l'eau dense le long de la côte italienne est complexe, influencé à la fois par l'eau intermédiaire et par la topographie du fond, en particulier dans les fosses du centre et du sud de l'Adriatique.

Oceanologica Acta, 1989, **12**, 2, 151-160.

INTRODUCTION

In this paper we use historical data stored in the "Yugoslav-Italian Data Base" at the Institute of Research on Marine Fisheries, C.N.R. (Ancona, Italy) and Institute of Oceanography and Fisheries (Split, Yugoslavia) to provide a picture of the formation and time-evolution of dense water in the Adriatic Sea (Fig. 1). We examined periods and places of formation, time evolution, influx into the Middle Adriatic Pit and outflow into the South Adriatic Pit of three different kinds of marine water, with $\sigma > 29.2$, 29.4 and 29.6 respectively (Pollak, 1951).

It is known that, during the winter season, the Adriatic Sea is strongly affected by the violence of the Bora, a cold, dry North-East wind (Zore-Armanda fully discusses this phenomenon and its different spatial effects, 1963). Consequently, the sea water cools and, owing to evaporation, its salinity increases. In the Northern Adriatic, this cooling is particularly noticeable owing both to the shallowness of this basin and to the strength of the Bora; on the other hand, owing to river runoff (particularly the Po river), salinity values remain somewhat low throughout the year. This cold and dense water then flows toward the Southern Adriatic, with a complex dynamics. On general grounds,

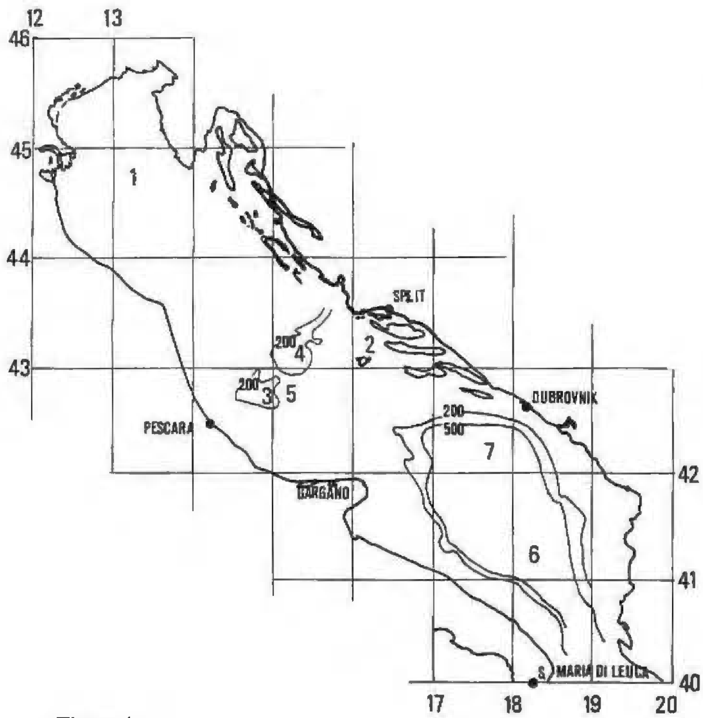

Figure 1

Geographical map and bathymetry (in metres) of the Adriatic Sea. Seven geographic regions (1/4 of Marsden square) are shown, in view of their importance for more detailed analyses.

Buljan's and Zore-Armanda's classical studies (1953; 1966; 1976) provide an interesting synthesis of the main hydrological characteristics of the Adriatic Sea. For more recent literature, *see* Franco *et al.* (1982).

In such a context, recent field observations of a vein of cold, bottom sea water ($\sim$ 30 km wide, 50 m deep) moving along the Italian coast are of particular interest: see Artegiani and Salusti (1988), for a review of many earlier field observations in the Middle Adriatic, and Zoccolotti and Salusti (1987), for measurements at the shelf break south of Gargano.

These works show that the dense water does not move from the Northern Adriatic Sea as a large, compact mass of water, in some sense like a marine avalanche (Fig. 2). On the contrary, it is observed as the quasi-steady bottom motion of a thin vein of dense water flowing southward, following quite faithfully the isobaths of the Italian coast. The fluxes were found to be $\Phi_M \simeq 2.10^4$ m^3/s in March, April 1981 in the Middle Adriatic, and $\Phi_N \simeq 10^4$ m^3/s, $\Phi_F \simeq 8.10^4$ m^3/s and $\Phi_J \simeq 6.10^4$ m^3/s in November 1980, February 1981, June 1983, respectively, at the shelf break south of Gargano.

The effect of the Bora is particularly evident in thermal satellite imagery showing averages of sea surface temperature, as may be seen in SATMER (1985; 1986). Two main cold patches in winter are of particular interest. The first can be observed in the Northern Adriatic during January-March; it subsequently evolves and forms a long coastal cold patch along the whole Italian coast. The second cold patch, very intense but not very long (some 50 km), can be observed from November to February along the Southern border of Yugoslavia (Champagne Philippe and Harong, 1982; Barale *et al.*, 1985), namely the Gulf of Drin.

These data can be fruitfully interpreted using our theoretical knowledge of motion, mixing and spreading of bottom veins of dense marine water: Shaw and Csanady (1984) describe the time-dependent motion of a bottom vein of dense water in a less dense stratified marine water. At first order, the dense water is shown to follow the isobaths rigorously, with a time propagation given by the classical Burger's equation (Whitham, 1974). For an initial dense water (*i. e.* denser than the environmental one), Shaw and Csanady (1984) show that the velocity of the front of this dense water is $v = V_0/\sqrt{t}$ for the time t. A numerical model based on these ideas, once applied to the Adriatic Sea, gives an average dense water velocity of 5 cm/s. The parameters are:

$$\begin{cases} S \simeq 10^{-3} \text{ is the bottom slope} \\ A \simeq 5.10^4 \text{ kg/m}^{-2} \text{ is the source excess mass} \\ \gamma \simeq 1{,}7.10^{-3} \text{ is the adimensionalized friction coefficient.} \end{cases}$$

In a different steady idealization, Smith (1975; *see* also Killworth, 1977) takes both diffusive and buoyant effects into account. Consequently his model can describe the entrainment due to the steady viscous buoyant motion of a vein of dense water on a sloping sea bottom. Its main results are that near the source the vein shows vertical oscillations; at a considerable distance (y) from the source, the steady motion is regular and densities and velocities decrease with y as $\sqrt{L/(y-y^*)}$. Conversely, the cross-shore section of the vein increases as $(y-y^*)/L$, while the angle between the vein and the isobaths (which is not zero since dissipative and viscous effects lower the vein motion) decreases as $\sqrt{L/(y-y^*)}$. The scale length $L \simeq 6$ km for the Adriatic Sea.

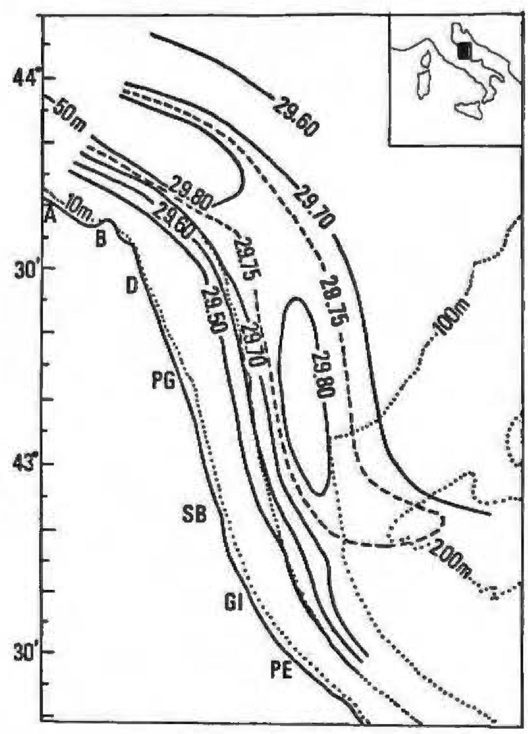

Figure 2

Bottom layer density along the Italian coast of the Central Adriatic, as measured during March 1981 (from Artegiani and Salusti, 1988).

Artegiani and Salusti (1988) applied this model to Middle Adriatic data and obtained a good agreement with an entrainment value of $\delta = 10^{-2}$.

In the following we first describe the synthesis of the historical hydrological data before extracting some working hypotheses that are further investigated by means of T−S diagrams. Since we discuss data relative to years characterized by widely differing climatological features for such a shallow basin, there is obviously a considerable annual variability. As we are more interested in climatological events than sporadic ones, we shall not discuss variances, confidence limits *etc.*, as in a classical data analysis, but will analyze the main features of the hydrological data. Some statistical aspects are discussed in the Appendix. The conclusions underline several new problems.

THE DATA SET: DENSITY MAPS

The data set of the "Yugoslav-Italian Data Base" used in this paper is based on more than 8000 hydrological stations from year 1911 to 1981, all referring to the Adriatic Sea. These stations are fairly regularly spread over the whole area, but the Northern Adriatic (NAS in the following) is more fully covered than the Middle (MAS in the following) and the Southern Adriatic (SAS in the following; Fig. 3). The Middle and Southern Adriatic coastal regions have been less regularly studied; in particular, the shelf break off Gargano is a little known area, which is particularly unfortunate. With regard to annual variability, year-by-year analyses of the entire Adriatic Sea are difficult to perform because of lack of sufficient information; we have therefore focused our attention on the main features of hydrological data in order to determine fundamental mechanisms to be used as key points in further discussions.

We start by examining the geographical distribution of those stations where, at some depth, a σ greater or equal to 29.6 has been found (Fig. 4). These stations are somewhat dense in the NAS in January and February, with a total number of 51 stations north of the 44th parallel. Inside the Middle Adriatic Pit (MAP, in the following) there are 3 stations, as many as on the Split-Gargano line. In March-April most of the NAS stations can be found further south, near the Italian coast. Around and inside the MAP there are now 26 stations and on the Split-Gargano line there are 6 stations. The flow at the southern border of the shelf is impossible to detect, since the shelf-break zone is unfortunately not covered by sufficient stations. After March-April this tendency continues: in the NAS, stations with $\sigma > 29.6$ gradually disappear, although some remain in the MAP and along the Split-Gargano line. This time-decrease in the number of stations continues also in December and new $\sigma > 29.6$ dense water is observable only in the next January-February period.

− The $\sigma > 29.4$ stations are much more numerous (Fig. 5). The same tendency in time can be observed. In January-February there are 130 NAS stations, 13 MAP stations and 4 Split-Gargano line stations. The same is true for the other periods of the year but near the Pelagosa Island, north of Gargano, dense-water stations are also very frequent. Inside the Southern Adriatic Pit (SAP in the following), dense water stations are very infrequent (1 in September-October, 3 in November-December).

− Stations with $\sigma > 29.2$ are more frequent all year round and display the same tendency (Fig. 6).

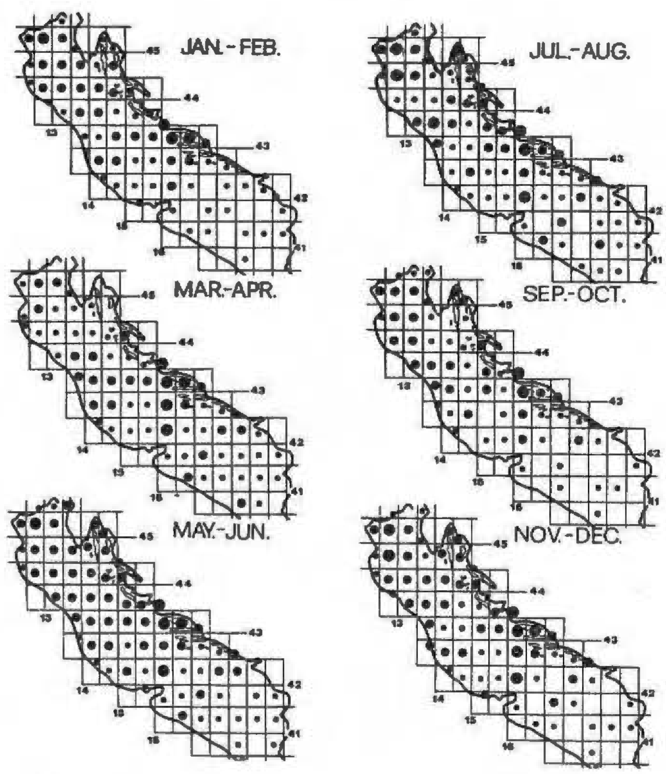

Figure 3

Geographical and temporal distribution of hydrological stations, in each geographical region (1/4 of Marsden square) and two-month periods. Large circles represent more than 50 stations, medium circles 11-50 stations, small circles less than 10 stations.

SALINITY MAPS

We now examine the time and space position of those stations whose salinity S is on at least one occasion higher than or equal to $S \geqq 38.8$, and 38.6, respectively. In January-February, stations with $S \geqq 38.8$ are frequent on the Split-Gargano line (10 stations) and along the Yugoslavian coast between Split and Dubrovnik. In NAS and in MAP, they have been found only in a few cases (3 and 2 respectively). The same happens throughout the year, with the sole exception of May-June, when the number of $S \geqq 38.8$ stations on the Split-Gargano line are comparable with those of MAP.

− The distribution of the $S \geqq 38.6$ stations resembles that of the $S \geqq 38.8$ case, but some stations can be found also in NAS. The Split-Gargano line is very rich in high salinity stations. These stations are again numerous in December. In the SAP, $S \geqq 38.6$ stations can be seen only after March-April.

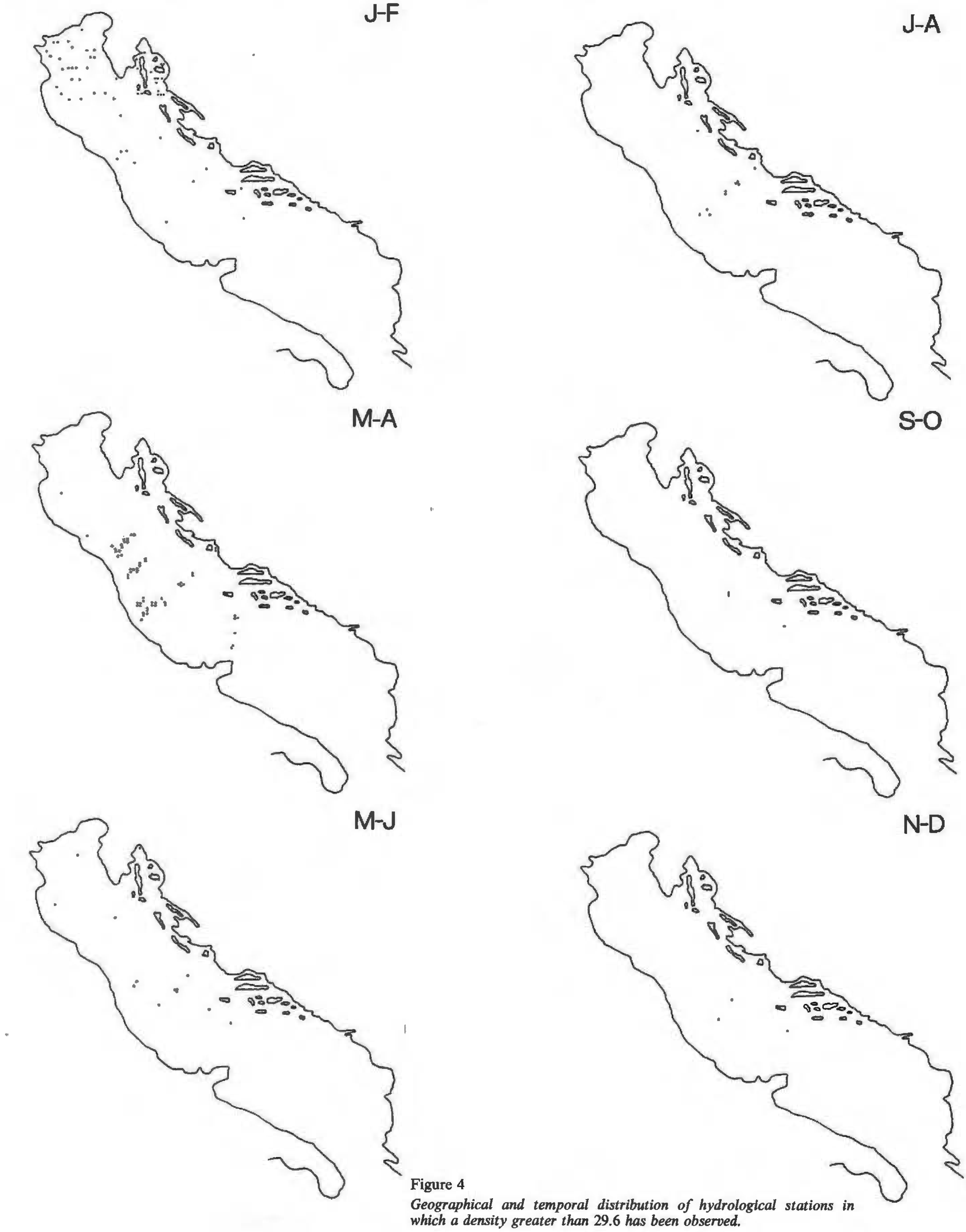

Figure 4
Geographical and temporal distribution of hydrological stations in which a density greater than 29.6 has been observed.

TEMPERATURE MAPS

The temperature plots show that stations with temperature T $\leq$ 10.2°C are frequent in NAS during January-February. Their number decreases in NAS during March-April and May-June. It is very interesting that only in July-August do they disappear completely. Conversely, their number increases in the MAP, showing the same southward movement as discussed above for the density field. Few of these stations can be found near the Yugoslavian coast.

We also plotted the cold-dense sea-waters, *i.e.* those $\sigma > 29.4$ waters that also had $T < 11.3$°C and $S < 38.4$. In this way we obtained the $\sigma \geqq 29.4$ waters whose density was mainly due to low temperature. These cold-dense waters were mainly localized in the northwestern part of the basin (Fig. 5, on the left of dark lines). It is also possible to define salty dense waters ($T \geqq 11.3$°C, $\sigma \geqq 29.4$, $S \geqq 38.4$). They showed the interesting feature of being localized also in the central part of NAS, but always south of 44°45'N (Fig. 5, on the right of the dark lines).

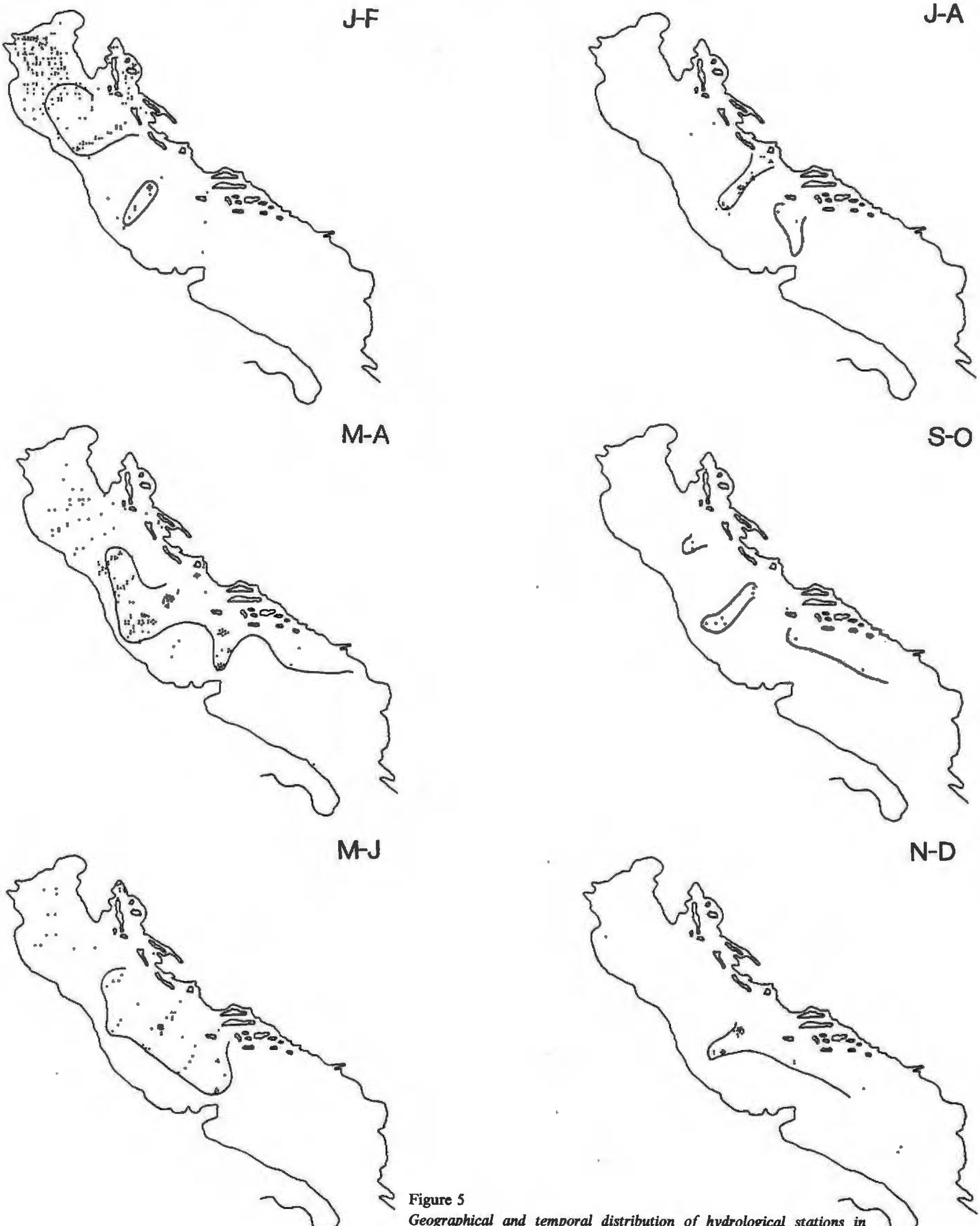

Figure 5

Geographical and temporal distribution of hydrological stations in which a density greater than 29.4 has been observed. The line separates stations with salinity greater than 38.4.

Figure 6
Geographical and temporal distribution of hydrological stations in which a density greater than 29.2 has been observed.

TEMPERATURE AND SALINITY OF THE BOTTOM WATER LAYERS

The preceding data suggest that the main source of the dense Adriatic Sea water is located in NAS. Moreover, very salty water can also be found in the Middle Adriatic near the Yugoslavian coast, even if its density is generally lower than that of NAS. The time-evolution of these components of dense water is now discussed in greater detail by examining T−S diagrams (Fig. 7) for some regions of particular interest (Fig. 1). As we are dealing with dense waters, we shall take into account only those waters whose density is $\sigma \geqq 29.2$.

The first region (#1) is in the middle of NAS. Its densest bottom water in the period November-June has $\sigma > 29.5$ and is rather cold ($\sim 10°C$). The second region (#2) is around Split. Its temperature is higher than in the preceding case, although the salinity values are so high that rather dense waters ($\sigma > 29.2$-29.3) can be found all year round. The third (#3) and fourth (#4) regions are, respectively, the western and the eastern part of MAP, where very high values of σ can be found ($\sigma > 29.7$). The T−S values are fairly constant throughout the year, due to the fact that the Pit can trap the sea-water masses. The water is saltier than in the NAS (#1) and colder than in the Split region (#2). This is very interesting, since it shows that both sources are important in MAP bottom-water feeding. On the saddle between MAP and SAP (region # 5), the T−S pattern is very similar to that in the western MAP, although the bottom water is a little fresher. This supports the idea that the MAP area is affected by important mixing processes involving more superficial water and that complex dynamical events must be present in that zone. In the middle of SAP (region #6), the water is among the warmest waters, being the most exposed to the Mediterranean warm water inflow. The T−S values are practically time-independent.

Figure 7

T−S diagrams of the densest water found in regions #1 to #6, in each of the six two-month periods of the year. The symbols A, B, C, D, E, F are indicative of the first, second, ... sixth of these two-monthly periods. Marine waters with $\sigma \leq 29.2$ are not considered as dense waters and have therefore been disregarded. Regions 1-6 are also shown.

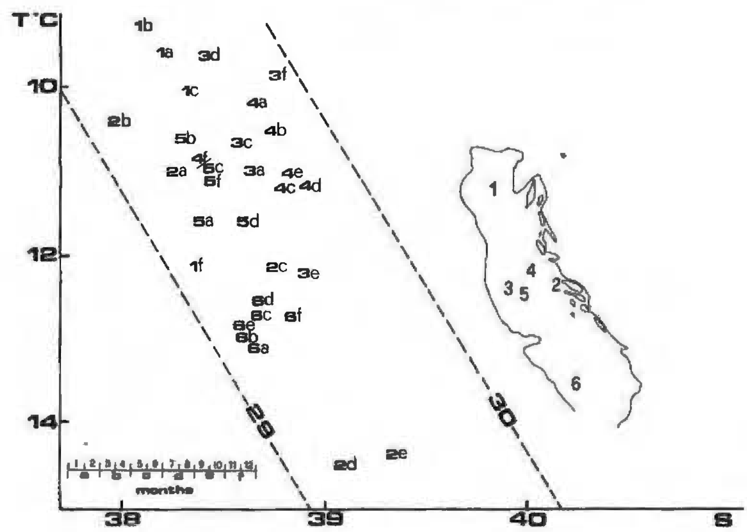

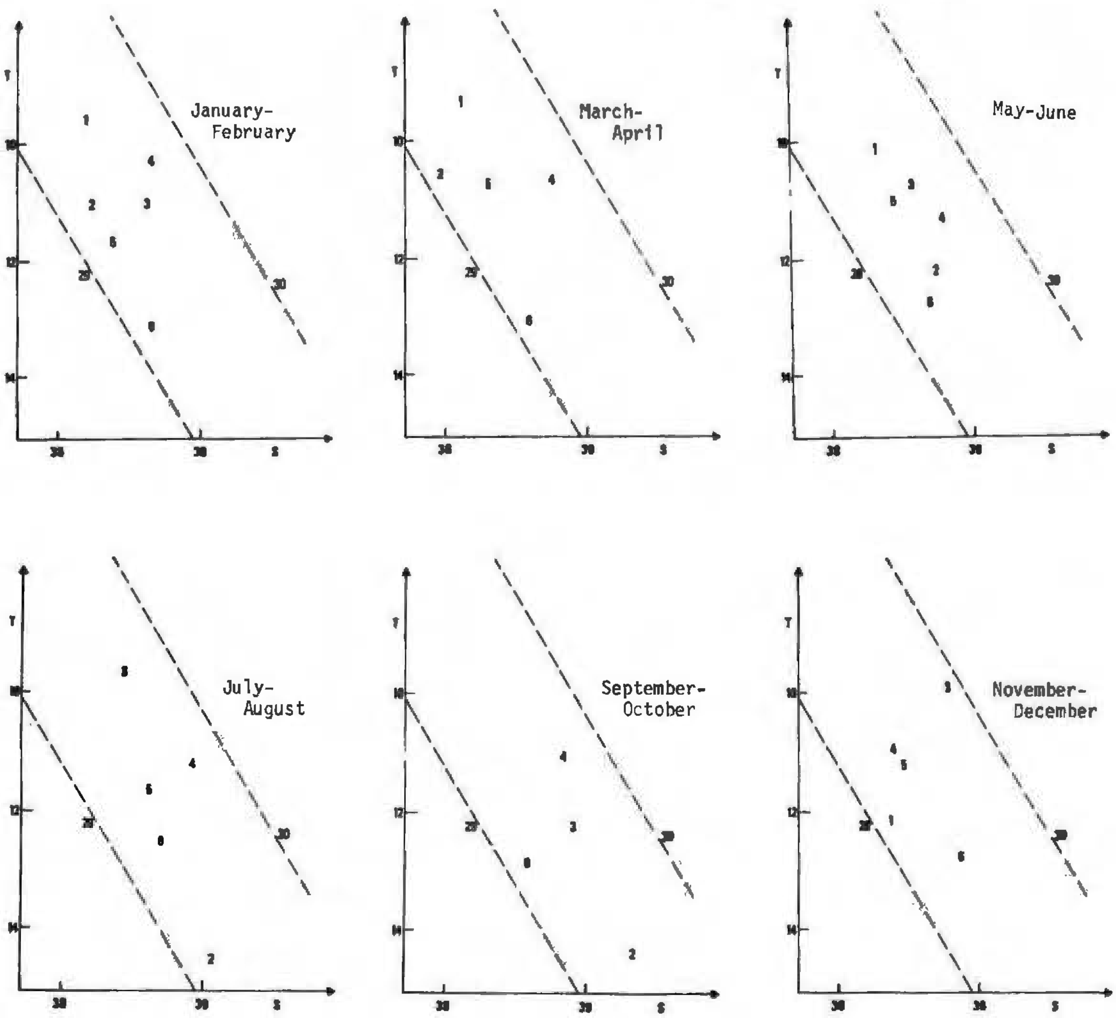

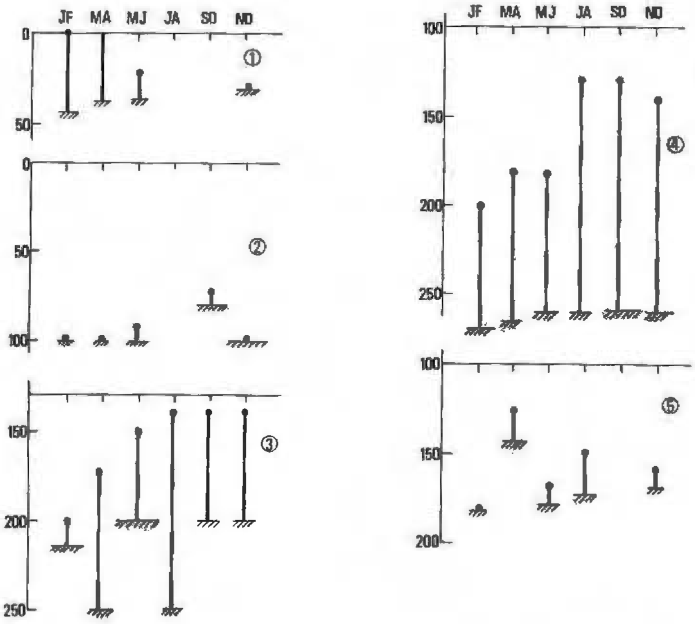

Figure 8

Graphic description of the σ ≧ 29.4 water layer greatest thickness (upper limit and bottom depth of the densest water observed), in regions #1 to #5, in each two-month period.

THICKNESS OF THE BOTTOM DENSE LAYER

For the same regions we also computed the greatest thickness of the σ ≧ 29.4 bottom water layers (Fig. 8). In January-April, in the NAS (#1), we often found layers 50 m thick, *i. e.* from the sea bottom to the surface. Near Split (#2) a 10-20 m thick layer is present also in summer on the bottom, at a depth of about 100 m. On the MAP (#3, #4), this bottom water is often present below a depth of 150 m, although in January-February its level is particularly low, ~ 200 m. This is in agreement with the idea that the dense water takes some months to enter the MAP. Lastly, in the saddle region (#5), there is always a layer from a depth of 150 m to the bottom, except in January and February when no evidence of this layer can be found.

TIME AND SPACE AVERAGED T−S DIAGRAMS

In the above considerations, only maximal values of temperature and salinity are considered, but transient phenomena could hide the quasi-steady flows. It is thus necessary to discuss time (two months) and space (1/4 of Marsden square) averaged values of T_b, S_b and σ_b, where "*b*" is the bottom depth.

In Figure 9 we show the T−S diagrams relative to bottom waters observed in the regions discussed in the preceding paragraph, plus a 7th region (#7) that seems of interest, located in the eastern part of the SAP (Fig. 1). The water of the NAS (#1, mean depth 35 m) and of the Split region (#2, mean depth 85 m) are well separated both for temperature and salinity. The two MAP regions (#3, mean depth 190 m and 4, mean depth 231 m) show little differences (the western part is a little warmer than the eastern one) and lie in the middle between the NAS and the SAP region waters (#6, #7), between the Split region (#2) water and NAS (#1) water. In the saddle region (#5, mean depth 158 m), marine waters show the same pattern as the eastern part of MAP but are found to be a little fresher. This confirms the ideas obtained from the preceding discussion of the T−S diagrams of extremal values. Lastly, regions #6 (mean depth 1050 m) and #7 (mean depth 1070 m) display very similar behaviour and are warmer and saltier than the MAP and NAS waters. The new region (#7) seems to be a little warmer and saltier than the others, in agreement with the idea that the inflow of warm and salty Mediterranean water follows the Yugoslavian coasts. Moreover, the density of these two last regions only occasionally reaches the values of the MAP and saddle region densities: the water masses over the shelf are generally denser than those found in deep layers of the Pits.

DISCUSSION

Our data show a complex pattern of the presence, time-evolution and diffusion of the dense Adriatic water; some general conclusions can however be drawn, to be considered as working hypotheses for further experiments and analyses.

Both experimental and theoretical results suggest that dense water motion is in agreement with the conservation of potential vorticity, *i. e.* the streamlines follow the isobaths to a large extent. This motion is anticlockwise because of the general circulation of the Adriatic Sea.

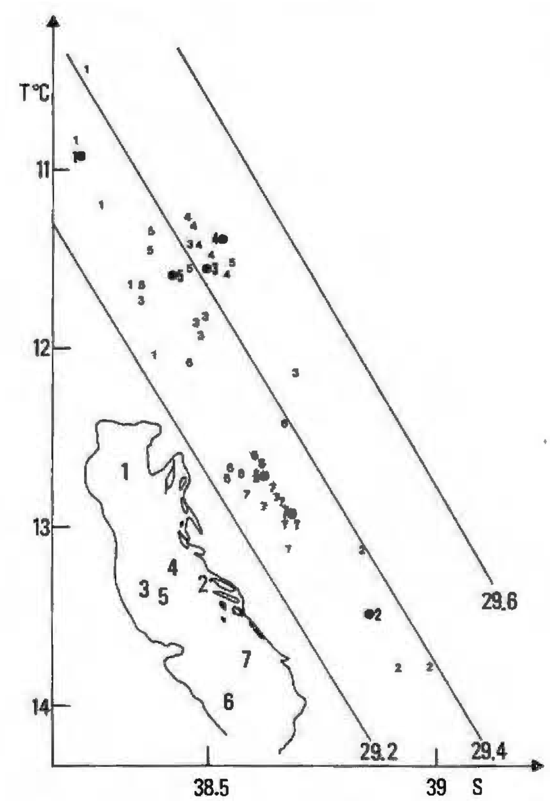

Figure 9

Time (over two-monthly periods) and space (over a 1/4 of Marsden square) average of bottom temperature and salinity for regions #1 to #7. Small points and small numbers are for a two-month period; large points and numbers refer to the whole year. We also show the classical values found by Zore-Armanda (1963).

The most important sources of $\sigma \geqq 29.4$ waters are in NAS (January-April). Another kind of marine water is important, namely the Intermediate water of Mediterranean origin, probably cooled by the Bora in wintertime. This Intermediate water is present in Southern and Middle Adriatic between 100 and 400 m; it has $T \sim 12.5°C$ and $S \sim 38.6$.

In order to illustrate more effectively the different time-evolutions of these two kinds of marine waters, we prefer to introduce an Intermediate water circulation model and a cold water circulation model. The cold water originates in the Northern Adriatic under the cooling effect of the Bora, which affects almost the whole water column. It remains there for a rather long time, probably trapped in the circulation of the NAS (water with $T < 10.2°C$ may be found until June, *see* Franco *et al.*, 1982). In the period March-April, part of this cold water moves southward along the Italian coast in apparent agreement with the conservation of potential vorticity. Theoretical considerations (Shaw and Csanady, 1984; Zoccolotti and Salusti, 1987) suggest that this water forms a well-defined vein (or rather a continuous set of blobs) of dense, cold water flowing alongshore at a depth of 50-150 m. It is of considerable interest that this theoretical idea has found experimental support (Artegiani *et al.*, 1988) in field observations near Pescara, between the Italian coast and the MAP (Fig. 2), and in field observations at the shelf break off Gargano (Zoccolotti and Salusti, 1987). It is of primary importance that the field observations confirm that this water can flow regularly along isobaths, without sinking completely into the MAP. Moreover we can see that, because of friction, a small part of slower and deeper water may often be observed further offshore and deeper than the main vein. Part of this water sinks into the MAP.

Moving further southward, this vein reaches the shelf break south of Gargano, producing a complex (buoyancy versus mixing) interaction, very similar to that observed in the tank experiment of Sugimoto and Whitehead (1983). In the field observations of Zoccolotti and Salusti (1987) a rough estimate of the flux of this water in about $10^4 - 10^5$ m^3/s can be found.

The evolution of the Intermediate water is also of particular interest. It is indeed possible to observe, even during August, a thin (10-20 m) layer of $\sigma \geqq 29.4$, $S \geqq 38.4$ in region 2, around Split. A possible reason for this effect is that this intermediate water is driven by the general cyclonic circulation of the Adriatic. Its densest part, being located at a depth of 60-80 m, cannot rise to shallower isobaths because of the potential vorticity conservation. Consequently it cannot flow further northward and is obliged to turn west following the isobaths of the eastern MAP. The lighter part of Intermediate water probably intrudes into the NAS. Comparison with T−S diagrams of the above regions enables us to identify the presence of this Intermediate water inside the bottom dense water of the Middle Adriatic Pit and suggests that the Intermediate water, during its cyclonic flow, interacts with the cold water, giving rise to the bottom water of the two lobes of MAP.

From this analysis a general model for dense water formation and evolution in the Adriatic Sea naturally emerges, as discussed in the previous pages. Its consequences on the sediments are of particular interest showing a natural agreement between regions where the dense water has been observed and bottom sediments. On the other hand, many fundamental problems arise: the continuity of the cold water vein and its stability are points to be studied in greater detail. Also the vertical diffusion of the dense water trapped inside the MAP is still an obscure, but fundamental phenomenon.

Appendix

The data were tested for consistency and coherence using standard techniques. To correct experimental errors, the Adriatic Sea was divided into quarters of Murdsen squares (*see* Fig. 1). For each region, mean and standard deviation has been calculated for all parameters at standard depth and for each month. Anomalous mean and standard deviation values indicate the existence of a possible error. It was thus possible to correct input errors; then the reliability of the measures was analyzed. This was a difficult task since, *a priori*, every datum must be considered true. On the other hand using different data obtained at different times, the pattern and sampling techniques must be adjusted. From this point of view, a mean and a confidence interval were calculated, which indicate, for a chosen probability level, the range of values inside which a new observation in the same period and region will fall.

The Adriatic Sea was divided into regions of around 12 square miles and the monthly mean and percentage standard deviation and number of stations were calculated. The mean percentage standard deviation and the standard error for each stratum of equal-sized station numbers were then calculated.

The results of this procedure, relative to temperature, are shown in Figure 10. The large dots represent the values of mean percentage standard deviation for every stratum. The small dots represent the confidence interval at 75% probability level. As may seen, the first part of diagrams (size 1-11) is strictly linear-dependent on the size of the strata ($r = 0.96$). The following data seem to be rather independent of the size of strata ($r = 0.04$), particularly for the largest sizes. On the other hand, the interpolating line of confidence interval is upper-limited so that an x-axis parallel straight line seems the best fitting, in accordance with theoretical considerations. The least-square method gives the following results:

a, b, and r values of the regression line $y = a + bx$

a) first part (size 2-11):
$a = 15.16$; $b = -0.58$; $r = 0.96$

b) second part (size 12-63):
$a = 9.92$; $b = 0$; $r = 0.04$

c) total (size 2-63):
$a = 11.22$; $b = -0.01$; $r = 0.15$

d) standard deviation (size 2-63):
$a = 6.78$; $b = 0$; $r = 0.02$.

The fitting-lines (*a*) and (*b*) are dashed in Figure 10. Theoretical considerations suggest that the *a*)-*b*) representation is more accurate than the (*c*) representation. The same theoretical considerations indicate that a possible continuous fitting curve could be an exponential, asymptotically converging to the $y = 9.68$ line.

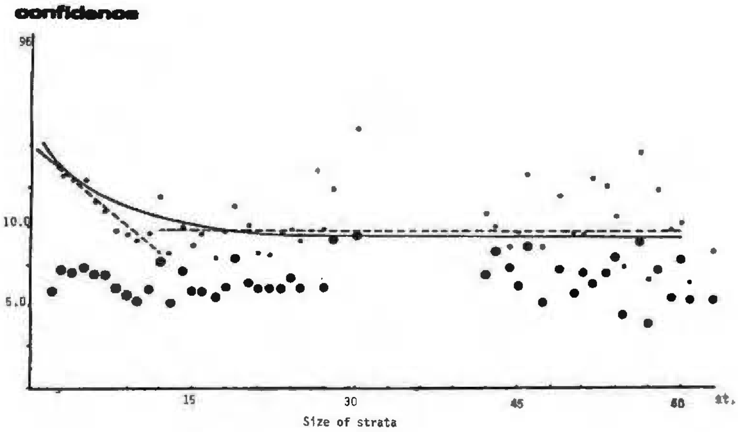

Figure 10

Confidence Interval of temperature values for strata. The size of the strata is on the abscissa; the percentage standard deviation of the strata (greater point) and the upper limit of the confidence interval at 70% level of the strata are on the ordinate. The dashed lines are the calculated regression lines for size 2-11 and 12-63. The continuous line is an interpolating curve representing the confidence interval as a function of the size of strata.

REFERENCES

Artegiani A. and E. Salusti (1988). Field observations of the flow of dense water on the bottom of the Adriatic Sea during the winter of 1981. *Oceanologica Acta*, **10**, 4, 387-391.

Barale V., M. Hendershott and P. M. Rizzoli (1985). Remotely sensing the surface dynamics of the Adriatic Sea. *Deep-Sea Res.*, **31**, 12, 1433-1459.

Buljan M. (1953). Fluctuations of salinity in the Adriatic. *Acta adriat.*, **2**, 2, 59 pp.

Buljan M. and M. Zore-Armanda (1966). Hydrographic data on the Adriatic sea collected in the period from 1952 through 1964. *Acta adriat.*, **12**, 438 pp.

Buljan M. and M. Zore-Armanda (1976). Oceanographical properties of the Adriatic Sea. *Oceanogr. Mar. Biol. ann. rev.*, **14**, 11-98.

Champagne Philippe M. and K. Harong (1982). Fronts thermiques superficiels en Méditerranée d'après les télémesures AVHRR. Note de travail n° 31, Ministère Français des Transports (unpublished).

Franco P., L. Jeftić, P. Malanotte, A. Michelato and M. Orlić (1982). A descriptive model of the Northern Adriatic. *Oceanologica Acta*, **5**, 3, 379-389.

Killworth P. (1977). Mixing on the Weddell sea continental slope. *Deep-Sea Res.*, **24**, 427-449.

Pollak M. J. (1951). The sources of the deep water of the Eastern Mediterranean Sea. *J. mar. Res.*, **10**, 128-152.

SATMER (1985). Revue de Météorologie Nationale, Lannion.

SATMER (1986). Revue de Météorologie Nationale, Lannion.

Shaw P. T. and G. T. Csanady (1984). Shelf-advection of density perturbation on a sloping continental shelf. *J. phys. Oceanogr.*, **13**, 769-782.

Smith P. C. (1975). A streamtube model for bottom boundary currents in the Ocean. *Deep-Sea Res.*, **22**, 853-673.

Sugimoto T. and J. Whitehead (1983). Laboratory models of bay-type continental shelves in Winter. *J. phys. Oceanogr.*, **13**, 10, 1819-1828.

Van Straten L. (1970). Holocene and late Pleistocene sedimentation in the Adriatic sea. *Geologische Rdsch.* **60**, 106-131.

Whitham A. (1974). *Linear and non-linear waves.* Wiley, New York, 615 pp.

Zoccolotti L. and E. Salusti (1987). Observations of a dense marine jet along the Southern Adriatic Sea. *Continent. Shelf. Res.*, **7**, 6, 535-551.

Zore-Armanda M. (1963). Les masses d'eau de la mer Adriatique. *Acta adriat.*, **10**, 3, 1-94.